Rewiring of Ancestral Cis-Regulatory Architecture Shapes Human Brain Evolution

Nilmini Hettiarachchi[1,*] , Gayan Prasad Hettiarachchi[2, 3]

[1]Faculty of Science, University of Colombo, 94 Kumaratunga Munidasa Mawatha, Colombo 00300, Sri Lanka

[2]Tokyo International University, 4-42-31 Higashi-Ikebukuro, Toshima, Tokyo, 170-0013 Japan

[3]R[3] Institute for Newly-Emerging Science Design, The University of Osaka, 1-2 Machikaneyama, Toyonaka, Osaka 560-0043, Japan

Corresponding author**:** Nilmini Hettiarachchi

Abstract

Understanding how human-specific brain traits emerged remains a central challenge in evolutionary biology. Although comparative genomic studies have identified numerous regulatory differences between humans and other primates, whether human brain evolution primarily reflects acquisition of novel regulatory elements or reorganization of ancestral cis-regulatory architecture remains unresolved. Here, we developed PRIME (Primate Regulatory Interaction Modeling of Enhancers), a quantitative framework integrating chromatin accessibility, transcriptional activity, and genomic distance to model evolutionary regulatory coordination at single-link resolution.

Using single-cell chromatin accessibility profiles from human, chimpanzee, and macaque brains across five major brain cell classes, we constructed a shared regulatory landscape comprising 364,657 consensus accessible chromatin regions and

23,812 linked genes. PRIME identified extensive human-specific regulatory rewiring despite broad conservation of global accessibility architecture. Human-reduced regulatory interactions substantially outnumbered human-increased interactions across most lineages, indicating that evolutionary divergence frequently reflects redistribution and reweighting of ancestral regulatory coordination.

Rewiring events were enriched within enhancer-associated regulatory elements but frequently occurred in promoter-overlapping and intragenic contexts, consistent with local cis-regulatory repurposing. Entropy analyses revealed lineage-specific redistribution of regulatory complexity, while H-DECI identified recurrent neuronal targets of coordinated human distal enhancer regulation. Matched-background null modeling confirmed 3.3–9.9-fold enrichment above expectation (FDR = 0.001), supporting regulatory rewiring and repurposing as major mechanisms of human brain evolution.

keywords: Human brain evolution, Cis-regulatory evolution, Enhancer rewiring, Chromatin accessibility, Regulatory network evolution

1. Introduction

The emergence of the human brain involved profound changes in cognition, language, social behavior, and neural plasticity, yet the molecular mechanisms underlying human-specific brain evolution remain incompletely understood. Comparative genomic studies have demonstrated that protein-coding divergence between humans and chimpanzees is relatively limited, suggesting that many uniquely human traits may instead arise from changes in gene regulation and cis-regulatory architecture rather than widespread invention of novel genes themselves (King and Wilson, 1975;

Pollard et al., 2006). Early comparative studies proposed that evolutionary changes in transcriptional regulation may represent a major driver of human phenotypic divergence, particularly in the nervous system (King and Wilson, 1975). Subsequent work identified large numbers of human accelerated regions (HARs), lineage-specific enhancers, and noncoding regulatory elements associated with neurodevelopmental processes and cortical expansion (Pollard et al., 2006; Capra et al., 2013; Guardiola-Ripoll et al., 2023).

Enhancers and other cis-regulatory elements are now recognized as central regulators of cell-type-specific transcriptional programs during brain development. Distal enhancer-promoter interactions (Hettiarachchi N., 2021; Hettiarachchi N., 2026), chromatin looping, transcription factor occupancy, and epigenetic remodeling collectively coordinate neuronal differentiation, synaptic maturation, gliogenesis, and activity-dependent plasticity (Hettiarachchi and Saitou., 2016). Advances in chromatin accessibility profiling and single-cell epigenomics have demonstrated that accessible chromatin landscapes are highly dynamic across developmental trajectories and cell states, providing critical insight into the regulatory logic underlying brain development and disease (Buenrostro et al., 2015; Corces et al., 2020; Li et al., 2023; Chen et al., 2024).

Recent studies further suggest that human brain evolution is associated with extensive remodeling of chromatin architecture and enhancer-promoter coordination. Comparative analyses of human accelerated regions and three-dimensional chromatin interactions indicate that many evolutionarily accelerated loci regulate conserved neurodevelopmental target genes rather than entirely novel pathways (Won et al., 2019; Pal et al., 2025). Similarly, studies of HAR-associated interactomes

demonstrate that human regulatory divergence may frequently emerge through altered coordination and rewiring of ancestral regulatory networks (Pal et al., 2025; Tan et al., 2025).

Importantly, increasing evidence suggests that evolutionary innovation does not necessarily require wholesale acquisition of entirely novel regulatory elements. Many conserved cis-regulatory regions retain broadly similar accessibility profiles across species while simultaneously exhibiting altered enhancer activity, transcription factor occupancy, developmental timing, or target-gene coordination (Reilly et al., 2015; Guardiola-Ripoll et al., 2023). Such findings support the emerging view that human brain evolution may frequently involve redistribution and functional repurposing of deeply conserved regulatory architecture rather than simple gain-or-loss of enhancer activity alone.

The human brain is especially likely to depend on such regulatory reorganization mechanisms because human neurodevelopment is characterized by prolonged developmental timing, delayed neuronal maturation, extended periods of synaptogenesis, and expanded windows of activity-dependent plasticity (Lui et al., 2011; Charrier et al., 2012; Lancaster, 2024). Inhibitory neuronal diversification, synaptic refinement, and glia-neuron coordination have emerged as particularly important contributors to human cortical specialization and cognitive complexity (Hodge et al., 2019; Bakken et al., 2021). Recent single-cell epigenomic studies additionally reveal extensive lineage-specific chromatin remodeling across neuronal and glial populations, suggesting that evolutionary rewiring is highly cell-type-dependent rather than uniformly distributed across the brain (Li et al., 2023).

Despite these advances, several major challenges remain unresolved. First, most comparative regulatory studies examine differential chromatin accessibility or differential gene expression independently rather than modeling coordinated regulatory interactions between accessible regulatory elements and transcriptional output. Second, many existing approaches conceptualize regulatory divergence primarily as binary gain-or-loss events, potentially overlooking subtler redistribution of regulatory coordination strength. Third, although single-cell technologies now permit lineage-resolved epigenomic analyses across species, quantitative frameworks capable of integrating chromatin accessibility, transcriptional activity, and regulatory topology into unified evolutionary interaction models remain limited.

To address these challenges, we developed PRIME (Primate Regulatory Interaction Modeling of Enhancers), a quantitative framework designed to model evolutionary cis-regulatory coordination across primate brain cell types. PRIME integrates chromatin accessibility, genomic distance architecture, and transcriptional activity into unified regulatory interaction scores that permit direct estimation of human-specific regulatory rewiring at single-link resolution. Rather than treating accessible chromatin regions as isolated elements, PRIME models regulatory architecture as coordinated interaction networks linking enhancer-like elements to transcriptional programs.

Using single-cell chromatin accessibility profiles from human, chimpanzee, and macaque brains across five major brain cell classes Microglia, Astrocytes, Excitatory neurons, Inhibitory neurons, and OPC/Oligodendrocyte-lineage cells we constructed a shared evolutionary regulatory landscape comprising 364,657 consensus accessible chromatin regions. We then quantified species-specific regulatory coordination

patterns, enhancer repurposing, regulatory entropy redistribution, and distal enhancer coordination architecture across lineages.

Our analyses reveal that human brain regulatory evolution is characterized by structured and highly lineage-specific cis-regulatory rewiring despite broad conservation of global chromatin accessibility landscapes. Surprisingly, human-specific rewiring frequently occurs within promoter-overlapping and intragenic enhancer-like regulatory regions rather than exclusively through highly distal enhancer innovation. We further identify widespread conserved-but-repurposed regulatory elements, redistribution of regulatory entropy, and strong neuronal distal enhancer coordination centered on neurodevelopmental and synaptic regulatory genes. These findings support a model in which human brain evolution emerged primarily through coordinated redistribution and functional rewiring of ancestral cis-regulatory landscapes rather than predominantly through acquisition of entirely novel regulatory systems.

2. Materials and Methods

2.1 Single-cell chromatin accessibility datasets and cross-species integration

Single-cell chromatin accessibility datasets (GSE192772) from human, chimpanzee, and macaque brain tissues were analyzed to investigate evolutionary cis-regulatory rewiring across major neural and glial lineages (Caglayan et al.2023). Five major brain cell classes were examined independently: Microglia, Astrocytes, Excitatory neurons, Inhibitory neurons, and OPC/Oligodendrocyte-lineage cells (OPCOli). All downstream analyses treated each cell type as an independent discovery dataset.

Chromatin accessibility profiles were represented as pseudobulk accessibility matrices generated from species-specific aggregated single-cell accessibility counts. To ensure direct evolutionary comparability across species, a shared consensus peak framework was constructed. Accessible regions from all species were merged into a unified nonredundant genomic interval set comprising 364,657 consensus accessible chromatin regions. All species- and cell-type-specific accessibility profiles were subsequently projected onto this shared peak coordinate system.

For each cell type and species, normalized pseudobulk accessibility values were computed for all consensus peaks. Peaks with insufficient accessibility signal across species were excluded from downstream evolutionary analyses.

2.2 Peak-to-gene assignment and regulatory interaction framework

Accessible chromatin regions were assigned to nearby genes using nearest-gene mapping based on genomic proximity to annotated transcription start sites (TSSs). For each accessible peak *e* and linked gene *g*, genomic distance was calculated as,

$$d_{e,g} = |m_e - t_g| \quad (1)$$

where $d_{e,g}$ denotes the genomic distance between peak *e* and gene *g*, m_e is the genomic midpoint coordinate of peak *e*, and t_g is the genomic coordinate of the transcription start site (TSS) of gene *g*. Peak midpoint coordinates were computed as,

$$m_e = s_e + e_e / 2 \quad (2)$$

where s_e and e_e denote the genomic start and end coordinates of peak e, respectively. Absolute genomic distance was measured in base pairs (bp).

Peak–gene relationships were retained across all genomic distances to permit analysis of both proximal and distal regulatory interactions. Because numerous regulatory elements overlap promoters, untranslated regions, and intragenic regions, many peak–gene assignments exhibited near-zero genomic distances. These assignments were retained because promoter-overlapping enhancers and intragenic regulatory elements constitute biologically relevant regulatory architectures in mammalian genomes and formed an important component of the regulatory repurposing patterns identified by PRIME.

2.3 PRIME framework for evolutionary regulatory interaction modeling

To quantify coordinated regulatory activity, we developed PRIME (Primate Regulatory Interaction Modeling of Enhancers), a quantitative framework integrating chromatin accessibility, transcriptional activity, and genomic distance into a unified regulatory interaction score.

For a regulatory element (e) linked to gene (g), the PRIME interaction score was defined as,

$$I_{e,g} = A_e * d_{e,g}^{-\alpha} \qquad (3)$$

where,

- $I_{e,g}$ denotes the regulatory interaction score between peak e and gene g
- A_e denotes normalized chromatin accessibility of regulatory element e

- $d_{e,g}$ represents genomic distance between peak e and the transcription start site (TSS) of linked gene g, as defined in Equation (1)
- α is a distance-decay exponent controlling the strength of distance penalization.

To incorporate transcriptional context, PRIME was extended to an expression-integrated formulation:

$$I_{e,g}^{PRIME} = A_e * E_g * d_{e,g}^{-\alpha} \qquad (4)$$

Where,

- $I_{e,g}^{PRIME}$ denotes the expression-integrated PRIME score
- E_g denotes normalized expression of linked gene g

This formulation enables simultaneous modeling of chromatin accessibility intensity, genomic regulatory distance, and coupling between accessible regulatory elements and transcriptional output.

Species-specific PRIME scores were computed independently for Human, Chimpanzee, and Macaque datasets, allowing direct comparison of regulatory interaction landscapes and estimation of human-specific regulatory rewiring.

2.4 Evolutionary PRIME shift estimation

To quantify human-specific regulatory rewiring, species-level PRIME scores were compared across primates. Human-versus-primate regulatory shift was calculated as,

$$\Delta I_{e,g} = I^{PRIME}_{Human,e,g} - \left(\frac{I^{PRIME}_{Chimp,e,g} + I^{PRIME}_{Macaque,e,g}}{2} \right) \quad (5)$$

Where,

- $\Delta I_{e,g}$ denotes the human-specific PRIME shift for regulatory element (e) linked to gene (g)
- $I^{PRIME}_{Human,e,g}$, $I^{PRIME}_{Chimp,e,g}$, $I^{PRIME}_{Macaque,e,g}$represent species-specific PRIME scores calculated independently for each species

Positive values of $\Delta I_{e,g}$ indicate increased regulatory coordination in humans relative to non-human primates, whereas negative values indicate reduced regulatory coordination in the human lineage.

For each cell type, empirical quantile thresholds of the absolute PRIME-shift distribution were used to define evolutionary rewiring events. Primary analyses employed a 95th percentile discovery threshold to identify directional rewiring, while 99th percentile thresholds were additionally evaluated for sensitivity analyses and characterization of extreme regulatory events.

Regulatory interactions were classified into three categories, Human-increased PRIME interactions, Human-reduced PRIME interactions, and Conserved or weakly shifted interactions.

2.5 Regulatory element annotation using ENCODE cCRE classifications

To characterize the regulatory architecture underlying PRIME rewiring, consensus peaks were annotated using ENCODE candidate cis-regulatory element (cCRE) annotations derived from the hg38 reference genome. Regulatory classes included, distal enhancer-like signatures (dELS), proximal enhancer-like signatures (pELS), promoter-like signatures (PLS),CTCF-associated regions, open chromatin regions, intragenic regions, promoter-proximal elements. Each consensus peak was assigned a final regulatory annotation category based on overlap with ENCODE cCRE coordinates. Overlap operations were performed using genomic interval intersection analyses. Regulatory class proportions and evolutionary enrichment patterns were subsequently quantified across all cell types and PRIME event classes.

2.6 Conserved, but repurposed regulatory element analysis

To identify regulatory elements exhibiting conserved accessibility but altered regulatory coordination, conserved-repurposed analyses were performed. Regulatory elements were classified as conserved if chromatin accessibility remained broadly similar across species, while simultaneously exhibiting substantial human-specific PRIME shifts. This framework enabled detection of regulatory repurposing events in which evolutionary divergence arises from altered coordination strength rather than accessibility gain or loss alone. Conserved-repurposed elements were further categorized into, conserved peaks with human-increased PRIME coordination, conserved peaks with human-reduced PRIME coordination, conserved peaks lacking strong PRIME rewiring.

2.7 Hub-gene rewiring analysis

To characterize higher-order regulatory coordination and identify focal points of evolutionary regulatory redistribution, gene-centered rewiring hubs were quantified independently within each brain cell type.

For each gene (g), regulatory interactions from all linked accessible elements were aggregated to compute hub-level rewiring statistics. The net rewiring score was defined as,

$$H_g = \sum_{e=1}^{ng} \Delta Ie, g \qquad (6)$$

Where,

- H_g denotes the cumulative rewiring score for gene (g)
- $\Delta Ie, g$ represents the evolutionary PRIME shift defined in Equation (5)
- (n_g) denotes the total number of regulatory elements linked to gene (g)

For each gene, additional hub descriptors were computed, including, total number of linked regulatory elements, number of human-increased PRIME interactions, number of human-reduced PRIME interactions, cumulative positive PRIME shift, cumulative negative PRIME shift, and net rewiring score. Genes exhibiting concentrated accumulation of coordinated PRIME interactions and large cumulative rewiring magnitude were classified as regulatory rewiring hubs. Hub rankings were computed independently for each cell type and subsequently compared across cell types to identify recurrent regulatory targets of human evolutionary divergence.

2.8 Regulatory entropy analysis

To quantify the distributional complexity of regulatory coordination, entropy-based analyses were performed for all genes linked to accessible regulatory elements. Regulatory entropy was used to measure how coordinated regulatory influence was distributed across multiple enhancer–gene interactions.

For a gene (g) linked to (n_g) regulatory elements, regulatory entropy was calculated as,

$$H_g = \sum_{i=1}^{n_g} p_i \log\left(p_i\right) \qquad (7)$$

where:

- H_g denotes regulatory entropy for gene (g)
- n_g denotes the total number of regulatory elements linked to gene (g)
- p_i represents the normalized contribution of regulatory element (i)

Normalized regulatory contribution probabilities were computed as,

$$p_i = \frac{\left|I_i\right|}{\sum_{j=1}^{n_g} \left|I_j\right|} \qquad (8)$$

where I_i denotes the PRIME interaction score associated with regulatory element (i), and the denominator represents the total regulatory contribution across all linked regulatory elements. Higher entropy values indicate distributed regulatory coordination across multiple regulatory elements, whereas lower entropy values indicate concentration of regulatory influence within a smaller number of interactions.

Species-specific entropy values were computed independently for Human, Chimpanzee, and Macaque datasets. Human-specific entropy redistribution was quantified relative to mean primate entropy as,

$$\Delta H_g = H_{Human} - \left(\frac{H_{Chimp} + H_{Macaque}}{2} \right) \quad (9)$$

where ΔH_g represents the human-specific regulatory entropy shift for gene (g). Genes were subsequently classified into three categories, human-expanded regulatory entropy ($\Delta H_g > 0$), human-contracted regulatory entropy ($\Delta H_g < 0$) and conserved entropy architecture (minimal entropy redistribution).

2.9 Human Distal Enhancer Coordination Index (H-DECI)

To specifically quantify coordinated human distal enhancer architecture, we developed the Human Distal Enhancer Coordination Index (H-DECI)**,** a composite gene-level metric designed to capture the magnitude and organization of human-specific distal enhancer coordination.

Only distal enhancer-like regulatory elements annotated as ENCODE enhancer-like distal signatures were included in H-DECI analyses.

For each gene (g), H-DECI was calculated as,

$$H\text{-}DECI_g = N_g * \overline{I^{PRIME}_{Human,g}} * \left(1 + H_g^{norm}\right) \quad (10)$$

Where,

- $H\text{-}DECI_g$ denotes the Human Distal Enhancer Coordination Index for gene (g)
- N_g is the number of linked human distal enhancer-like regulatory elements
- $\overline{I^{PRIME}_{Human,g}}$ is the mean Human PRIME score across distal enhancer links associated with gene (g)
- H_g^{norm} denotes normalized distal enhancer entropy.

Normalized entropy was calculated as:

$$H_g^{norm} = \frac{H_g}{\log(N_g)} \qquad (11)$$

where (H_g) is the regulatory entropy defined in Equation (7), and $\log(N_g)$ represents the theoretical maximum entropy for a gene linked to (N_g) distal enhancer elements.

This formulation jointly captures enhancer multiplicity, coordinated human regulatory activity, and distributional complexity of distal enhancer organization. Genes with elevated H-DECI values were interpreted as exhibiting coordinated human-active distal enhancer regulation and were considered candidate focal points of human regulatory specialization.

2.10 Matched-background null modeling

To assess the statistical robustness of PRIME rewiring, matched-background permutation analyses were performed to determine whether observed regulatory shifts exceeded expectations derived from comparable regulatory interactions. Observed human-shifted PRIME interactions were compared against randomly sampled background regulatory links matched simultaneously for, regulatory class, genomic

distance, chromatin accessibility intensity, and transcriptional activity. Background regulatory links were stratified into multidimensional matching bins constructed using regulatory annotation category, distance-to-gene architecture, accessibility quantiles, and expression quantiles to preserve local regulatory structure. For each cell type and rewiring class, empirical null distributions were generated through repeated matched-background permutation sampling. Observed cumulative PRIME shift and mean PRIME shift statistics were subsequently compared against null distributions to estimate empirical significance.

Empirical p-values were calculated as:

$$p = \frac{N_{null \geq observed} + 1}{N_{perm} + 1} \quad (12)$$

Where,

- p denotes the empirical permutation p-value
- $N_{null \geq observed}$ represents the number of null permutations producing values greater than or equal to the observed statistic
- N_{perm} denotes the total number of permutation iterations.

Multiple testing correction was performed using the Benjamini–Hochberg procedure to estimate false discovery rates (FDR).

2.11 Distance-shift analyses

To investigate spatial regulatory architecture, genomic distance distributions were examined across PRIME event classes and regulatory annotations. Because many biologically relevant regulatory elements overlap promoters or intragenic regions,

analyses were interpreted in the context of local regulatory repurposing rather than exclusively distal enhancer relocation. Distance analyses included, density distribution comparisons, distance-bin enrichment analyses, regulatory-class-specific distance architectures, PRIME-shift-versus-distance relationships.

2.12 Functional enrichment analysis

Gene ontology (GO) enrichment analyses were performed for genes associated with human-increased and human-reduced PRIME rewiring events.

Enrichment analyses were conducted separately for each cell type using biological process annotations. Functional categories associated with neuronal differentiation, synaptic signaling, chromatin regulation, immune signaling, and developmental pathways were subsequently examined.

2.13 Statistical analyses and visualization

All computational analyses were performed in R (V 4.5.2). Data manipulation utilized dplyr and data.table frameworks, while genomic interval analyses were performed using Bioconductor genomic range utilities. Statistical visualization employed ggplot2.

Permutation-based significance testing utilized empirical matched-background null distributions. Unless otherwise specified, all reported significance values correspond to empirical permutation-derived p-values adjusted using false discovery rate correction.

3. Results

3.1 Cross-species chromatin accessibility landscapes reveal widespread conservation with selective human-specific divergence across brain cell types

To investigate the evolutionary organization of cis-regulatory architecture across the primate brain, we analyzed pseudobulk chromatin accessibility profiles derived from human, chimpanzee, and macaque single-cell ATAC-seq datasets spanning five major brain cell classes: Microglia, Astrocytes, Excitatory neurons, Inhibitory neurons, and OPC/Oligodendrocyte-lineage cells (OPCOli). A shared regulatory framework consisting of 364,657 consensus accessible chromatin regions was constructed and used across all downstream analyses (Figure 1). Dataset composition and accessibility characteristics for all cell types are summarized in Table 1.

Across all lineages, the majority of accessible chromatin regions exhibited broadly conserved accessibility patterns, indicating substantial preservation of regulatory architecture across primate brain evolution. Nevertheless, selective human-specific accessibility divergence was evident in every cell type, although the magnitude of divergence varied considerably between lineages.

Excitatory neurons exhibited the strongest accessibility divergence, with 24,544 peaks (6.73% of all accessible regions) displaying human-reduced accessibility relative to the primate background. Astrocytes, Microglia, OPC/Oligodendrocyte-lineage cells, and Inhibitory neurons also exhibited substantial numbers of human-reduced accessibility events, comprising 18,232 (5.00%), 18,040 (4.95%), 17,157 (4.70%), and 14,427 (3.96%) peaks, respectively (Figure2, Table 2). In contrast, human-gained accessibility events were comparatively uncommon across all cell types, ranging from 0.03% to 0.36% of accessible regions.

The predominance of human-reduced accessibility events across multiple neural and glial lineages suggests that evolutionary divergence of chromatin architecture is characterized primarily by selective redistribution and refinement of ancestral accessibility landscapes rather than widespread acquisition of novel accessible regulatory regions. These observations establish a conserved chromatin accessibility framework within which subtler forms of regulatory rewiring can subsequently be examined.

3.2 PRIME reveals asymmetric human-specific regulatory rewiring across brain cell types

To quantify evolutionary changes in regulatory coordination beyond chromatin accessibility alone, we developed PRIME (Primate Regulatory Interaction Modeling of Enhancers), a framework that integrates chromatin accessibility, genomic distance, and transcriptional activity into unified regulatory interaction scores. PRIME enables direct comparison of peak–gene regulatory coordination across species and provides a quantitative measure of human-specific regulatory rewiring at single-link resolution (Figure 1).

At the 95th percentile empirical threshold, human-specific regulatory rewiring was strongly asymmetric across all five cell types, with human-reduced regulatory interactions consistently outnumbering human-increased interactions (Figure 3; Table 3). Microglia exhibited 18,040 human-reduced and 193 human-increased PRIME interactions, whereas Astrocytes contained 18,232 reduced and only a single increased interaction. Excitatory neurons displayed 18,233 reduced interactions with no detectable increased interactions above threshold, while Inhibitory neurons and

OPC/Oligodendrocyte-lineage cells exhibited 17,702 and 17,157 reduced interactions accompanied by 531 and 1,076 increased interactions, respectively.

These findings indicate that evolutionary divergence of regulatory coordination is not balanced between gain and loss processes. Instead, human regulatory evolution appears dominated by selective attenuation, redistribution, and reorganization of pre-existing regulatory interactions, with only a relatively small subset of interactions exhibiting enhanced human-specific coordination.

3.3 Matched-background null modeling confirms that PRIME rewiring substantially exceeds regulatory expectations

To determine whether observed PRIME rewiring patterns could arise from generic properties of accessible chromatin or gene architecture, we implemented a matched-background null framework controlling for regulatory class composition, chromatin accessibility intensity, transcriptional activity, and genomic distance structure. Observed human-shifted PRIME interactions were compared with matched regulatory background distributions using cumulative and mean PRIME-shift statistics (Figure 4; Table 4).

Across all analyzed brain cell types, observed PRIME rewiring magnitudes substantially exceeded matched null expectations. Human-reduced rewiring displayed particularly strong enrichment relative to matched background regulatory interactions. Microglia showed the strongest relative enrichment, with observed cumulative PRIME shift exceeding matched null expectation by 9.88-fold. OPC/Oligodendrocyte-lineage cells and Inhibitory neurons also showed strong enrichment, with null enrichment ratios of 7.98 and 5.96, respectively. Excitatory

neurons displayed the largest absolute cumulative rewiring magnitude overall, with 2536.817 cumulative PRIME shift units, corresponding to 3.26-fold enrichment relative to matched background distributions (Table 4).

Human-increased rewiring events were comparatively less frequent but still enriched above matched null expectations in multiple lineages. OPC/Oligodendrocyte-lineage cells showed 5.14-fold enrichment for human-increased PRIME rewiring, while Microglia showed 4.65-fold enrichment. In contrast, Astrocyte human-increased rewiring exhibited weaker enrichment (1.62-fold), consistent with the observation that Astrocytes showed only a single human-increased PRIME event at the 95% threshold (Table 4).

Empirical permutation testing demonstrated that observed rewiring patterns exceeded matched null expectations across all major event classes, with empirical FDR = 0.000999 for cumulative PRIME-shift enrichment. The findings here indicate that PRIME rewiring reflects structured evolutionary redistribution of cis-regulatory coordination rather than simple biases in accessibility intensity, promoter proximity, expression magnitude, or regulatory-element class composition.

3.4 Human-specific regulatory rewiring preferentially targets locally repurposed cis-regulatory architecture

To characterize the regulatory architecture underlying PRIME rewiring, we annotated the shared cross-species ATAC peak landscape using ENCODE candidate cis-regulatory element (cCRE) classifications. The 364,657 consensus accessible chromatin regions were assigned to regulatory classes including distal enhancer-like,

proximal enhancer-like, promoter-like, promoter-proximal, CTCF-like, intragenic, open chromatin, and distal candidate cis-regulatory categories (Figure 5A; Table 5).

Across the shared peak landscape, enhancer-associated regulatory elements represented the largest annotated component. Distal enhancer-like elements accounted for 147,865 peaks (40.55%), while proximal enhancer-like elements accounted for an additional 13,110 peaks (3.60%). Intragenic regulatory regions represented 110,110 peaks (30.20%), followed by distal candidate cis-regulatory elements (53,864 peaks; 14.77%), promoter-like elements (17,505 peaks; 4.80%), CTCF-like elements (13,314 peaks; 3.65%), open chromatin regions (4,858 peaks; 1.33%), and promoter-proximal regions (4,031 peaks; 1.11%) (Figure 5A; Table 5). Collectively, enhancer-associated and intragenic regulatory elements comprised more than 74% of all shared accessible regions, indicating that the conserved primate brain regulatory landscape is dominated by enhancer-like and intragenic architecture rather than promoter-associated elements alone.

We next examined whether human-specific PRIME rewiring events preferentially occurred within particular regulatory classes. At the 95% empirical discovery threshold, directional PRIME events were strongly enriched within enhancer-like regulatory contexts across multiple cell types (Figure 5B–C; Table 6). Human-increased PRIME events in Microglia were dominated by enhancer-like elements, with distal and proximal enhancer-like classes comprising 58.55% of increased links. Inhibitory neurons showed an even stronger enhancer-centered pattern, with enhancer-like elements accounting for 68.18% of human-increased PRIME events, while OPC/Oligodendrocyte-lineage cells displayed 65.99% enhancer-like composition among human-increased events. Human-reduced PRIME events also

showed substantial enhancer-like representation across lineages, generally ranging from approximately 48% to 53% of all rewiring events (Figure 5C; Table 6).

Importantly, PRIME rewiring was not restricted to distal enhancer-like regions. Promoter-associated and intragenic regulatory contexts also contributed substantially to the rewiring landscape, particularly among human-reduced events (Figure 5B). These findings indicate that human-specific regulatory evolution is not adequately described by a simple model of distal enhancer gain. Rather, regulatory divergence involves coordinated redistribution across enhancer-like, promoter-associated, and intragenic accessible regulatory elements.

Consistent with this interpretation, genomic distance analyses demonstrated that many high-PRIME rewiring events occurred within promoter-overlapping or intragenic regulatory contexts, generating numerous peak–gene assignments with near-zero genomic distance. Rather than indicating a lack of regulatory complexity, this pattern suggests that human-specific regulatory evolution frequently operates through local repurposing of accessible cis-regulatory architecture, including promoter-proximal and intragenic enhancer-like elements. Along with the strong enrichment of enhancer-associated cCRE annotations, these observations support a model in which human brain regulatory evolution is driven largely by redistribution and functional rewiring of pre-existing accessible regulatory landscapes rather than by widespread acquisition of entirely novel distal enhancers.

To determine whether evolutionary divergence primarily reflected new accessibility states or altered utilization of conserved regulatory architecture, we examined conserved-but-repurposed PRIME links. Across all major brain cell types, conserved accessible regions frequently exhibited substantial human-specific changes in

regulatory coordination despite showing little or no accessibility divergence (Figure 6B; Table 7). Conserved-repurposed events were overwhelmingly dominated by human-reduced PRIME coordination, with approximately 3,500–3,700 conserved-repurposed reduced links detected in each major lineage. Human-increased conserved-repurposed interactions were comparatively rare but remained detectable, particularly in Microglia and OPC/Oligodendrocyte-lineage cells (Figure 6B).

3.5 Entropy redistribution and hub-gene rewiring reveal coordinated remodeling of human brain regulatory networks

3.5.1 Entropy redistribution

To investigate higher-order regulatory organization beyond individual regulatory interactions, we quantified gene-centered regulatory entropy across species. Regulatory entropy captures the distribution of coordinated regulatory influence across enhancer–gene networks and provides a measure of regulatory complexity at the gene level. Across all major brain cell types, entropy architecture was highly conserved, with approximately 95% of genes classified as evolutionarily stable in regulatory complexity (Table 8). Nevertheless, distinct subsets of genes exhibited substantial human-specific redistribution of regulatory coordination.

Analysis of regulatory entropy revealed widespread reorganization of human regulatory coordination landscapes across cell types (Figure 6A). Although the majority of genes retained conserved entropy structure, subsets of genes exhibited marked expansion or contraction of coordinated regulatory influence, indicating selective remodeling of enhancer–gene coordination networks despite overall conservation of regulatory architecture.

Entropy expansion was considerably more common than entropy contraction across all lineages (Figure 6A; Table 8). Excitatory neurons and inhibitory neurons displayed the largest numbers of entropy-expanded genes (990 and 993 genes, respectively), whereas Microglia exhibited 693 entropy-expanded genes and 498 entropy-contracted genes. OPC/Oligodendrocyte-lineage cells also showed extensive entropy expansion (911 genes) relative to contraction (275 genes). These findings indicate that human regulatory evolution frequently increases the diversity of coordinated regulatory inputs affecting individual genes rather than reducing network complexity.

Genes exhibiting entropy expansion were enriched for regulators involved in neuronal development, chromatin organization, and cell-state coordination. Representative entropy-expanded genes included PDGFRA, SLX4IP, TFEC, RERGL, and TECRL, each of which gained broader distributions of coordinated regulatory influence in the human lineage. In contrast, entropy-contracted genes included GNG7, ARHGAP39, ADGRB1, NTN1, and PAX5, suggesting lineage-specific consolidation of regulatory control around a more restricted set of interactions (Table 8).

Collectively, these findings indicate that human regulatory evolution is associated with selective redistribution of enhancer-mediated regulatory complexity rather than wholesale restructuring of regulatory networks. While the overall architecture of regulatory coordination remains highly conserved, a restricted subset of genes undergoes substantial expansion or contraction of coordinated regulatory influence, providing a potential substrate for lineage-specific regulatory innovation.

3.5.2 Hub gene rewiring

To identify focal points of coordinated regulatory remodeling, we next examined recurrent hub genes exhibiting strong PRIME rewiring across multiple cell types. Several genes emerged as highly recurrent rewiring centers, including DLG2, PDE4D, TCF4, TRIO, DST, ARID1B, FOXP1, ZEB2, MAGI1, and SND1 (Figure 7; Table 9). Notably, many of these genes are established regulators of neuronal differentiation, synaptic organization, axon guidance, and higher-order cognitive function. The recurrence of these genes across multiple brain lineages suggests that human regulatory evolution preferentially targets conserved developmental and neuronal control nodes rather than acting uniformly across the genome.

The strongest recurrent hub-like organization was observed within neuronal populations, particularly inhibitory and excitatory neurons, where extensive coordinated rewiring converged on genes such as DLG2, PDE4D, TCF4, and TRIO (Figure 7). In contrast, Microglia exhibited a more restricted rewiring architecture characterized by fewer highly connected hubs and greater concentration within immune-neural coordination pathways. These observations indicate that human brain evolution is associated with selective redistribution of regulatory complexity around lineage-specific network hubs rather than pervasive genome-wide rewiring.

Collectively, the entropy and hub-gene analyses reveal a common organizational principle of human regulatory evolution: evolutionary divergence is concentrated within a limited set of highly connected regulatory nodes that undergo substantial redistribution of coordinated enhancer influence while the broader regulatory architecture remains largely conserved. These observations raised the possibility that a subset of genes may act as focal points of coordinated enhancer-mediated regulatory organization across multiple cell types.

3.6 Human distal enhancer coordination converges on neurodevelopmental and synaptic regulatory genes

To directly quantify coordinated human-active distal enhancer architecture, we developed the Human Distal Enhancer Coordination Index (H-DECI), a composite metric integrating the number of linked distal enhancer-like regulatory elements, cumulative human PRIME activity, and entropy-normalized enhancer coordination distribution. H-DECI was designed to identify genes that function as focal points of coordinated human-specific distal enhancer regulation rather than simply exhibiting individual high-scoring regulatory interactions (Figure 8; Table 10).

Substantial differences in distal enhancer coordination architecture were observed across brain cell types (Table 10). Inhibitory neurons exhibited the strongest coordinated distal enhancer landscape (mean H-DECI = 0.285), followed by excitatory neurons (0.177) and OPC/Oligodendrocyte-lineage cells (0.176). Astrocytes (0.062) and Microglia (0.045) displayed comparatively lower overall distal enhancer coordination, indicating that large-scale coordinated enhancer architecture is concentrated primarily within neuronal lineages.

Despite these lineage-specific differences, a remarkably consistent set of genes emerged as recurrent targets of human distal enhancer coordination across multiple brain cell types (Figure 8; Table 11). The strongest recurrent H-DECI genes included DLG2, PDE4D, TCF4, TRIO, DST, ARID1B, FOXP1, ZEB2, MAGI1, and SND1. Notably, all ten genes were identified among the top-ranked coordinated enhancer targets in all five major brain cell classes. These genes are well-established regulators

of neuronal differentiation, synaptic organization, axon guidance, chromatin remodeling, and higher-order neurodevelopmental processes, suggesting that human regulatory evolution converges on a common set of developmental control nodes.

Cell-type-specific H-DECI profiles further revealed distinct regulatory coordination programs (Supplementary Table 1). Astrocytes exhibited coordinated distal enhancer architecture centered on genes including NAV2, NFIB, PDE4D, TCF4, PRKCH, ANK2, DST, and TRIO. In contrast, inhibitory neurons displayed particularly strong coordination around synaptic and signaling-associated genes such as PDE4D, DLG2, PTPRD, FOXP1, TCF4, and TRIO. Similar patterns were observed in excitatory neurons and OPC/Oligodendrocyte-lineage cells, where recurrent enhancer coordination converged on genes implicated in neuronal connectivity, circuit formation, and synaptic plasticity.

The magnitude of coordinated distal enhancer architecture was substantial. Across cell types, approximately 85,000–88,000 human distal enhancer interactions contributed to H-DECI calculations, with 8,695–8,765 genes participating in coordinated enhancer networks (Table 10). Recurrent H-DECI genes frequently accumulated more than 100 linked distal enhancer interactions while simultaneously exhibiting among the highest enhancer coordination scores observed in the study (Figure 8).

Collectively, these findings indicate that human regulatory evolution is not characterized by diffuse enhancer innovation across the genome. coordinated distal enhancer activity converges on a relatively restricted set of neurodevelopmental, synaptic, and transcriptional regulatory genes that repeatedly emerge as focal points of enhancer-mediated regulatory organization across independent brain cell lineages.

The recurrence of these targets across neuronal, glial, and immune-associated populations suggests that human regulatory evolution preferentially remodels a conserved core of developmental control genes rather than generating lineage-specific regulatory innovations in isolation.

4. Discussion

Our analyses support a model in which human brain evolution emerged primarily through rewiring and repurposing of ancestral cis-regulatory architecture rather than widespread acquisition of entirely novel regulatory systems. In this study, we developed PRIME, a quantitative framework for modeling evolutionary cis-regulatory coordination across primate brain cell types by integrating chromatin accessibility, genomic distance architecture, and transcriptional activity into a unified regulatory interaction model. Across five major neural and glial lineages, PRIME revealed extensive human-specific regulatory rewiring despite broad conservation of overall chromatin accessibility architecture. Importantly, our results consistently indicate that human brain regulatory evolution is characterized less by wholesale emergence of novel regulatory systems and more by redistribution, reweighting, and coordinated repurposing of pre-existing cis-regulatory landscapes.

A central finding of this study is that human-specific rewiring was strongly asymmetric across cell types and regulatory directions. Human-reduced regulatory interactions substantially outnumbered human-increased interactions across nearly all lineages, with particularly strong effects observed in Microglia, inhibitory neurons, and OPC/Oligodendrocyte-lineage cells. This pattern suggests that evolutionary

divergence in the human brain may not primarily involve simple additive accumulation of regulatory activity, but rather selective refinement and redistribution of ancestral regulatory coordination networks. Such a model aligns with growing evidence that human brain evolution involved extensive developmental tuning of pre-existing mammalian regulatory architectures rather than widespread creation of entirely novel genes or pathways.

Our analyses further revealed that many high-PRIME rewiring events occurred within promoter-overlapping or intragenic regulatory regions rather than exclusively within highly distal enhancer landscapes. While distal enhancer innovation has often been emphasized in models of human brain evolution, our findings support a more locally coordinated regulatory framework in which promoter-proximal enhancers, intragenic enhancer-like elements, and compact accessible chromatin architectures play major roles in lineage-specific regulatory divergence. This interpretation is consistent with recent evidence demonstrating that enhancer-promoter boundaries are frequently fluid, that intragenic enhancers contribute substantially to neuronal transcriptional regulation, and that many active mammalian regulatory elements function within highly compact chromatin interaction neighborhoods.

The strong enrichment of conserved-but-repurposed regulatory elements further supports this interpretation. Numerous regulatory elements retained broadly conserved accessibility across primates while simultaneously exhibiting substantial human-specific PRIME shifts. Such patterns suggest that evolutionary innovation can emerge through altered coordination strength and redistribution of existing regulatory relationships rather than accessibility gain or loss alone. This mechanism may provide

an efficient evolutionary strategy for modifying transcriptional programs while preserving core developmental and cellular regulatory architecture.

Entropy analyses further revealed that human brain evolution involved selective redistribution of regulatory coordination complexity rather than uniform expansion of regulatory architecture. Although most genes retained conserved entropy structure across species (~95% across all analyzed cell types), distinct subsets exhibited either expanded or contracted regulatory entropy in humans, indicating lineage-specific remodeling of coordinated enhancer–gene influence. Expanded entropy states frequently corresponded to genes with more distributed enhancer coordination patterns, suggesting broader allocation of regulatory contribution across multiple regulatory elements. Conversely, entropy contraction may reflect increased concentration, stabilization, or canalization of regulatory influence.

Notably, the balance between entropy expansion and contraction differed across cellular lineages. Neuronal populations displayed the strongest enrichment of entropy-expanded genes, consistent with broader redistribution of regulatory coordination and increased organizational flexibility of enhancer architecture. In contrast, Astrocytes exhibited a comparatively distinct profile, with fewer entropy-expanded genes (676) and more entropy-contracted genes (515) than Microglia (693 expanded; 498 contracted). This pattern suggests that human astrocyte evolution may involve selective concentration and refinement of regulatory coordination rather than broad expansion of regulatory complexity. Such restructuring supports a model in which evolutionary innovation can emerge through redistribution and reweighting of existing regulatory influence within conserved cis-regulatory landscapes rather than through widespread acquisition of additional regulatory interactions.

These findings suggest that human brain evolution involves lineage-specific remodeling of regulatory coordination topology, with neuronal lineages favoring broader coordination landscapes and glial populations exhibiting more selective redistribution of regulatory control.

One of the most striking findings of the study was the strong distal enhancer coordination architecture observed in neuronal lineages, particularly inhibitory neurons. Human distal enhancer coordination converged on genes including DLG2, PDE4D, TCF4, TRIO, ARID1B, FOXP1, and ZEB2, many of which are centrally involved in synaptic organization, neurodevelopment, neuronal differentiation, and neuropsychiatric disease. The prominence of inhibitory neuronal rewiring is especially intriguing given increasing evidence that inhibitory interneuron diversification and prolonged synaptic maturation contributed substantially to human cortical specialization. Human cortical development is characterized by extended developmental timing, prolonged synaptogenesis, delayed neuronal maturation, and expanded windows of activity-dependent plasticity. Coordinated distal enhancer regulation may therefore represent a mechanism for stabilizing long developmental trajectories while simultaneously enabling flexible transcriptional modulation across extended developmental periods.

The comparatively weaker enhancer coordination observed in Microglia and Astrocytes may also carry important evolutionary implications. Microglia exhibited highly significant but relatively localized rewiring patterns enriched for selective hub-like coordination rather than globally distributed enhancer expansion. This may reflect the strong evolutionary constraint acting on innate immune regulatory systems, where excessive regulatory divergence could disrupt conserved neuroimmune

homeostasis. Astrocytes similarly displayed weaker human-increased rewiring signals, suggesting that some glial lineages may maintain comparatively conserved regulatory architectures despite participating in broader human brain specialization.

Importantly, matched-background null modeling demonstrated that observed PRIME rewiring substantially exceeded expectations generated from regulatory-class-, accessibility-, expression-, and distance-matched null distributions. In several lineages, cumulative rewiring magnitude exceeded matched null expectation by more than five- to ten-fold. These findings indicate that the observed evolutionary patterns cannot be explained simply by accessibility intensity, promoter proximity, or regulatory annotation composition alone, but instead reflect structured redistribution of regulatory coordination architecture.

Collectively, our results support a model in which human brain evolution emerged through coordinated remodeling of ancestral cis-regulatory systems rather than predominantly through acquisition of entirely novel regulatory elements. In this framework, evolutionary innovation is achieved by selectively redistributing regulatory influence, altering enhancer coordination topology, and modulating cell-type-specific regulatory entropy within pre-existing accessible chromatin landscapes. Such a mechanism may provide both evolutionary flexibility and developmental stability, enabling substantial functional divergence while preserving core regulatory organization required for mammalian brain development.

Several limitations should be considered. Peak-to-gene assignment relied primarily on nearest-gene relationships and did not explicitly incorporate three-dimensional chromatin interaction data. Future integration with Hi-C, promoter-capture Hi-C, or single-cell multiomic datasets may further refine regulatory interaction architecture.

In addition, although pseudobulk accessibility provides robust lineage-level regulatory estimation, finer-grained developmental trajectory analyses may reveal additional transient or state-specific evolutionary rewiring events. Finally, functional perturbation experiments will ultimately be required to validate the causal regulatory effects predicted by PRIME.

The present study establishes a generalizable framework for modeling evolutionary regulatory coordination at single-cell resolution. Beyond primate neurobiology, PRIME may provide a broadly applicable strategy for investigating evolutionary rewiring across tissues, developmental systems, and disease states. More broadly, our findings suggest that one of the defining features of human brain evolution may not be the creation of entirely novel regulatory architecture, but rather the coordinated redistribution of ancestral regulatory landscapes into uniquely human developmental and neuronal programs.

Conflict of Interest

The author declares no conflict of interest.

Funding

No external funding was received for this work.

Author contributions

N.H conceived the research topic, performed the computational and statistical analyses, synthesized and interpreted the scientific findings, prepared the figures and

tables, and wrote and revised the manuscript. G.P.H contributed with valuable comments, statistical methods, applications and editing of the manuscript.

Ethics statement

This manuscript is an original research article based on published datasets. No new experiments involving human participants, animals, or clinical data were conducted by the author. Consequently, ethical approval and informed consent were not required.

Data availability statement

Data and scripts can be made freely available upon request.

References

Bakken, T.E., Jorstad, N.L., Hu, Q., et al. (2021). Comparative cellular analysis of motor cortex in human, marmoset and mouse. Nature, 598, 111–119.

Buenrostro, J.D., Wu, B., Chang, H.Y. and Greenleaf, W.J. (2015). ATAC-seq: A method for assaying chromatin accessibility genome-wide. Current Protocols in Molecular Biology, 109, 21.29.1–21.29.9.

Caglayan, E., Ayhan, F., Liu, Y., Vollmer, R.M., et al. (2023). Molecular features driving cellular complexity of human brain evolution. Nature, 620(7972), 145–153.

Capra, J.A., Erwin, G.D., McKinsey, G., et al. (2013). Many human accelerated regions are developmental enhancers. Philosophical Transactions of the Royal Society B: Biological Sciences, 368, 20130025.

Charrier, C., Joshi, K., Coutinho-Budd, J., et al. (2012). Inhibition of SRGAP2 function by its human-specific paralogs induces neoteny during spine maturation. Cell, 149, 923–935.

Chen, Y., Li, H., Wang, J., et al. (2024). Chromatin accessibility: Biological functions, molecular mechanisms, and disease relevance. Signal Transduction and Targeted Therapy, 9, 203.

Corces, M.R., Shcherbina, A., Kundu, S., et al. (2020). Single-cell epigenomic analyses implicate candidate causal variants at inherited risk loci for Alzheimer's and Parkinson's diseases. Nature Genetics, 52, 1158–1168.

Guardiola-Ripoll, M., Rodríguez-Santiago, B. and Girirajan, S. (2023). A systematic review of the human accelerated regions in neurodevelopment and cognition. Genome Biology and Evolution, 15, evac196.

Hettiarachchi, N. and Saitou, N. (2016). GC content heterogeneity in conserved noncoding sequences. Genome Biology and Evolution, 8(11), 3377–3392.

Hettiarachchi, N. (2021). Primate deep conserved noncoding sequences and non-coding RNA. iDarwin, 2, 3–33.

Hettiarachchi N. (2026). Regulatory Evolution and the Genetic Basis of Human Brain Expansion. J Mol Evol, 94(5):761-784. doi: 10.1007/s00239-026-10344-1. Epub 2026 Sep 6. PMID: 42701979.

Hodge, R.D., Bakken, T.E., Miller, J.A., et al. (2019). Conserved cell types with divergent features in human versus mouse cortex. Nature, 573, 61–68.

King, M.C. and Wilson, A.C. (1975). Evolution at two levels in humans and chimpanzees. Science, 188, 107–116.

Lancaster, M.A. (2024). Unraveling mechanisms of human brain evolution. Cell, 187, 5319–5334.

Li, Y.E., Preissl, S., Hou, X., et al. (2023). A comparative atlas of single-cell chromatin accessibility in the human brain. Science, 382, eadf7044.

Lui, J.H., Hansen, D.V. and Kriegstein, A.R. (2011). Development and evolution of the human neocortex. Cell, 146, 18–36.

Pal, A., Nowakowski, T.J., Ahituv, N., et al. (2025). Resolving the three-dimensional interactome of human accelerated regions in neural stem cells. Cell, 188, 1021–1039.

Pollard, K.S., Salama, S.R., Lambert, N., et al. (2006). An RNA gene expressed during cortical development evolved rapidly in humans. Nature, 443, 167–172.

Reilly, S.K., Yin, J., Ayoub, A.E., et al. (2015). Evolutionary changes in promoter and enhancer activity during human corticogenesis. Science, 347, 1155–1159.

Tan, K., Wilkinson, M.F., et al. (2025). An ancient enhancer rapidly evolving in the human lineage promotes neural progenitor formation. Science Advances, 11, eadi1234.

Won, H., Huang, J., Opland, C.K., et al. (2019). Human evolved regulatory elements modulate genes involved in cortical expansion and neurodevelopmental disease susceptibility. Nature Communications, 10, 2396.

Global Scientific JOURNALS

Table 1. Summary of primate brain cell-type datasets and chromatin accessibility profiles. Summary of the five major brain cell classes analyzed across human, chimpanzee, and macaque single-cell chromatin accessibility datasets. A shared framework of 364,657 consensus accessible chromatin regions was constructed and used throughout all downstream analyses. Mean and median accessibility values represent pseudobulk chromatin accessibility estimates across the consensus peak landscape. Collectively, the dataset comprised 56,043 cells spanning neuronal, glial, immune, and oligodendroglial lineages, providing a comprehensive framework for investigating evolutionary regulatory divergence across the primate brain.

Cell Type	Species	Cells (n)	Consensus Accessible Peaks	Mean Accessibility	Median Accessibility
Microglia	Human	676	364,657	0.0169	0.0074
	Chimpanzee	1,406	364,657	0.0200	0.0064
	Macaque	1,680	364,657	0.0211	0.0060
Astrocyte	Human	2,874	364,657	0.0199	0.0125
	Chimpanzee	1,038	364,657	0.0370	0.0202
	Macaque	280	364,657	0.0329	0.0179
Excitatory Neuron	Human	9,903	364,657	0.0466	0.0324
	Chimpanzee	7,435	364,657	0.0547	0.0328
	Macaque	6,511	364,657	0.0502	0.0252
Inhibitory Neuron	Human	3,331	364,657	0.0305	0.0216
	Chimpanzee	3,389	364,657	0.0339	0.0207
	Macaque	2,607	364,657	0.0349	0.0184
Oligodendrocyte Lineage (OPC)	Human	8,191	364,657	0.0187	0.0084
	Chimpanzee	5,275	364,657	0.0283	0.0078
	Macaque	11,446	364,657	0.0232	0.0066

Table 2. Human-specific chromatin accessibility divergence across major primate brain cell types. Accessible chromatin regions were classified according to cross-species accessibility differences among human, chimpanzee, and macaque

pseudobulk ATAC-seq profiles. Conserved or small-change peaks represent regions exhibiting no substantial human-specific accessibility divergence. Human-gained peaks denote regions with increased accessibility in the human lineage relative to non-human primates, whereas human-reduced peaks represent regions with decreased accessibility in humans. Percentages are reported relative to the shared set of 364,657 consensus accessible chromatin regions used throughout the study. Across all cell types, the majority of accessible regions remained evolutionarily conserved (>92%), while human-specific divergence was dominated by accessibility reduction rather than widespread acquisition of novel accessible regions. Excitatory neurons exhibited the greatest accessibility divergence, whereas inhibitory neurons showed the highest degree of conservation.

Cell Type	Conserved or Small-Change Peaks	Human-Gained Accessibility Peaks	Human-Reduced Accessibility Peaks	Conserved (%)	Human-Gained (%)	Human-Reduced (%)
Microglia	346,424	193	18,040	94.99	0.05	4.95
Astrocyte	346,424	1	18,232	95.00	0.00	5.00
Excitatory Neuron	338,810	1,303	24,544	92.91	0.36	6.73
Inhibitory Neuron	350,129	101	14,427	96.02	0.03	3.96
OPC	346,424	1,076	17,157	95.00	0.30	4.70

Table 3. Human-specific PRIME rewiring events identified at the 95% empirical discovery threshold. PRIME (Primate Regulatory Interaction Modeling of Enhancers) scores were used to quantify species-specific regulatory coordination between accessible chromatin regions and their associated target genes. Human-increased PRIME links represent regulatory interactions exhibiting stronger coordinated accessibility–expression relationships in humans relative to chimpanzee

and macaque, whereas human-reduced PRIME links represent interactions exhibiting weaker coordination in the human lineage. Directional rewiring events were defined using the 95th percentile empirical PRIME-shift threshold. Across all brain cell types, human-reduced regulatory interactions substantially outnumbered human-increased interactions, indicating that human regulatory evolution is characterized primarily by redistribution and attenuation of existing regulatory coordination rather than widespread acquisition of novel regulatory interactions. OPC/Oligodendrocyte-lineage cells exhibited the largest number of human-increased rewiring events, whereas excitatory neurons displayed exclusively human-reduced interactions at this stringent discovery threshold.

Cell Type	Human-Increased PRIME Links	Human-Reduced PRIME Links	Total Directional PRIME Links	Human-Increased (%)	Human-Reduced (%)
Microglia	193	18,040	18,233	1.06	98.94
Astrocyte	1	18,232	18,233	0.01	99.99
Excitatory Neuron	0	18,233	18,233	0.00	100.00
Inhibitory Neuron	531	17,702	18,233	2.91	97.09
OPC	1,076	17,157	18,233	5.90	94.10

Table 4. Matched-null validation of human-specific PRIME rewiring effect sizes. Observed PRIME rewiring events were compared against biologically matched null distributions controlling for chromatin accessibility, transcriptional activity, genomic distance, and regulatory-element class. The Null Enrichment Ratio (NER) quantifies the magnitude of observed rewiring relative to matched-null expectation. Across all major brain cell types, observed PRIME rewiring substantially exceeded matched-null

expectations, with enrichment ranging from 3.26-fold to 9.88-fold for human-reduced interactions and 1.62-fold to 5.14-fold for human-increased interactions, supporting structured evolutionary redistribution of cis-regulatory coordination.

Cell Type	Event	Observed Events	Observed Cumulative PRIME Shift	Null Cumulative Shift	NER	Z score	FDR
Microglia	Human-reduced	18,040	997.929	100.955	9.88	1751.02	0.000999
OPC	Human-reduced	17,157	1236.887	154.982	7.98	1349.42	0.000999
Inhibitory Neuron	Human-reduced	17,702	828.761	138.941	5.96	951.17	0.000999
Astrocyte	Human-reduced	18,232	1694.860	387.151	4.38	970.09	0.000999
Excitatory Neuron	Human-reduced	18,233	2536.817	778.763	3.26	724.31	0.000999
OPC	Human-increased	1,076	45.123	8.772	5.14	187.37	0.000999
Microglia	Human-increased	193	4.413	0.948	4.65	71.69	0.000999
Inhibitory Neuron	Human-increased	531	13.641	3.979	3.43	77.20	0.000999
Astrocyte	Human-increased	1	0.038	0.023	1.62	1.54	0.000999

Table 5. Regulatory annotation of the shared cross-species accessible chromatin landscape. Consensus accessible chromatin regions (n = 364,657) were annotated using ENCODE candidate cis-regulatory element (cCRE) classifications. Distal enhancer-like elements represented the largest regulatory category, followed by intragenic and distal candidate cis-regulatory regions, indicating that the shared

primate brain regulatory landscape is dominated by enhancer-associated and intragenic accessible architecture rather than promoter-associated elements alone.

Regulatory class	Number of peaks	Percentage (%)
Distal enhancer-like	147,865	40.55
Intragenic	110,110	30.20
Distal candidate CRE	53,864	14.77
Promoter-like	17,505	4.80
CTCF-like	13,314	3.65
Proximal enhancer-like	13,110	3.60
Open chromatin	4,858	1.33
Promoter-proximal	4,031	1.11

Table 6. Enhancer-like composition of human-specific PRIME rewiring events at the 95% empirical discovery threshold. Human-specific PRIME rewiring events were classified according to their underlying regulatory annotation to quantify the contribution of enhancer-associated architecture to regulatory redistribution. Values indicate the proportion of directional PRIME events occurring within distal and proximal enhancer-like regulatory elements. NA indicates that no human-increased PRIME events were detected at the selected discovery threshold and therefore enhancer composition could not be estimated.

Cell type	Human-increased (%)	Human-reduced (%)
Microglia	58.55	52.00
Astrocyte	NA	53.00
Excitatory Neuron	NA	52.00
Inhibitory Neuron	68.18	50.00
OPC	65.99	48.00

Table 7. Conserved accessible regions exhibiting human-shifted PRIME coordination. Conserved-repurposed regulatory links represent accessible chromatin regions that remained broadly conserved across primate species but exhibited substantial human-specific changes in PRIME regulatory coordination. Human-increased links indicate strengthened regulatory coordination in the human lineage,

whereas human-reduced links indicate attenuation of coordinated regulatory influence despite preserved accessibility.

Cell type	Conserved human-increased links	Conserved human-reduced links
Microglia	3	3600
Excitatory	0	3647
Inhibitory	0	3643
OPC	61	3579

Table 8. Human-specific redistribution of regulatory entropy across major primate brain cell types.
Regulatory entropy quantifies the distribution of coordinated enhancer–gene influence and serves as a measure of gene-centered regulatory complexity. Conserved genes retained similar entropy structure across species, whereas entropy-expanded and entropy-contracted genes exhibited increased or reduced distributions of coordinated regulatory influence in the human lineage, respectively. Across all cell types, entropy conservation remained dominant, while a subset of genes showed selective redistribution of regulatory coordination consistent with human-specific network remodeling.

Cell type	Conserved genes	Entropy-expanded genes	Entropy-contracted genes
Microglia	22,621	693	498
Excitatory	22,300	990	201
Inhibitory	22,300	993	198
OPC	22,000	916	275
Astrocyte	22,621	676	515

Table 9. Recurrent human distal enhancer coordination genes across brain cell types.
Recurrent human distal enhancer coordination genes identified across major brain cell types using the Human Distal Enhancer Coordination Index (H-DECI). H-DECI integrates distal enhancer abundance, coordinated human PRIME activity, and enhancer coordination distribution to quantify gene-centered distal regulatory

organization. Maximum H-DECI indicates the strongest observed coordination score for a gene in any single cell type, whereas Total H-DECI represents cumulative coordinated distal enhancer influence across all represented cell types. The recurrence of these genes across all five major brain lineages suggests that human regulatory evolution converges on a conserved set of neurodevelopmental and synaptic regulatory hubs rather than acting uniformly across the genome.

Gene	Cell types represented	Maximum H-DECI	Total H-DECI
DLG2	5	17.5	42.8
PDE4D	5	17.2	38.8
TCF4	5	12.8	35.8
TRIO	5	15.0	31.6
DST	5	8.3	24.8
ARID1B	5	8.6	21.5
SND1	5	8.8	21.2
FOXP1	5	7.4	20.3
ZEB2	5	6.5	17.1
MAGI1	5	5.8	15.2

Table 10. Cell-type summary of human distal enhancer coordination architecture quantified using the Human Distal Enhancer Coordination Index (H-DECI). H-DECI integrates the number of linked distal enhancer-like elements, coordinated human PRIME activity, and entropy-normalized enhancer coordination to measure gene-centered distal regulatory organization. Mean and median H-DECI summarize the overall strength of coordinated enhancer regulation within each cell type, while the top H-DECI gene identifies the strongest coordinated distal enhancer target. Neuronal lineages exhibited the strongest enhancer coordination architecture,

indicating preferential concentration of human distal regulatory organization within neurodevelopmental and synaptic regulatory programs. (Supplementary Table 1)

Cell type	Genes with distal enhancer links	Total distal enhancer links	Mean H-DECI	Median H-DECI	Top H-DECI gene
Inhibitory	8,765	87,910	0.285	0.044	PDE4D
Excitatory	8,765	87,910	0.177	0.030	DLG2
OPC	8,765	87,910	0.176	0.018	DLG2
Astrocyte	8,765	87,900	0.062	0.007	NAV2
Microglia	8,695	85,339	0.045	0.005	FRMD4A

Table 11. Recurrent human distal enhancer coordination genes identified across major brain cell types using the Human Distal Enhancer Coordination Index (H-DECI). Maximum H-DECI represents the strongest observed distal enhancer coordination score for a gene within a single cell type, whereas Total H-DECI reflects cumulative coordinated enhancer influence across all represented lineages. The recurrence of these genes across all five brain cell classes indicates that human regulatory evolution preferentially converges on a conserved set of neurodevelopmental, synaptic, and transcriptional regulatory hubs.

Gene	Cell types represented	Maximum H-DECI	Total H-DECI
DLG2	5	17.5	42.8
PDE4D	5	17.2	38.8
TCF4	5	12.8	35.8
TRIO	5	15.0	31.6
DST	5	8.3	24.8
ARID1B	5	8.6	21.5
SND1	5	8.8	21.2
FOXP1	5	7.4	20.3
ZEB2	5	6.5	17.1
MAGI1	5	5.8	15.2

Figure 1. Overview of the PRIME framework for identifying human-specific regulatory rewiring across primate brain cell types. The workflow integrates single-cell ATAC-seq and RNA-seq information from human, chimpanzee, and macaque across five major brain cell classes to construct a shared cross-species regulatory landscape. Accessible chromatin profiles were processed through pseudobulk aggregation, peak–gene assignment, and expression integration to compute PRIME scores that combine chromatin accessibility, transcriptional activity, and genomic distance into a unified regulatory coordination metric. Downstream analyses quantified human-specific regulatory rewiring, conserved regulatory repurposing, entropy redistribution, distal enhancer coordination (H-DECI), and matched-null enrichment to identify evolutionary restructuring of cis-regulatory

architecture. Collectively, the framework supports a model in which human brain evolution is driven predominantly by redistribution and repurposing of ancestral accessible regulatory elements rather than widespread emergence of entirely novel regulatory states.

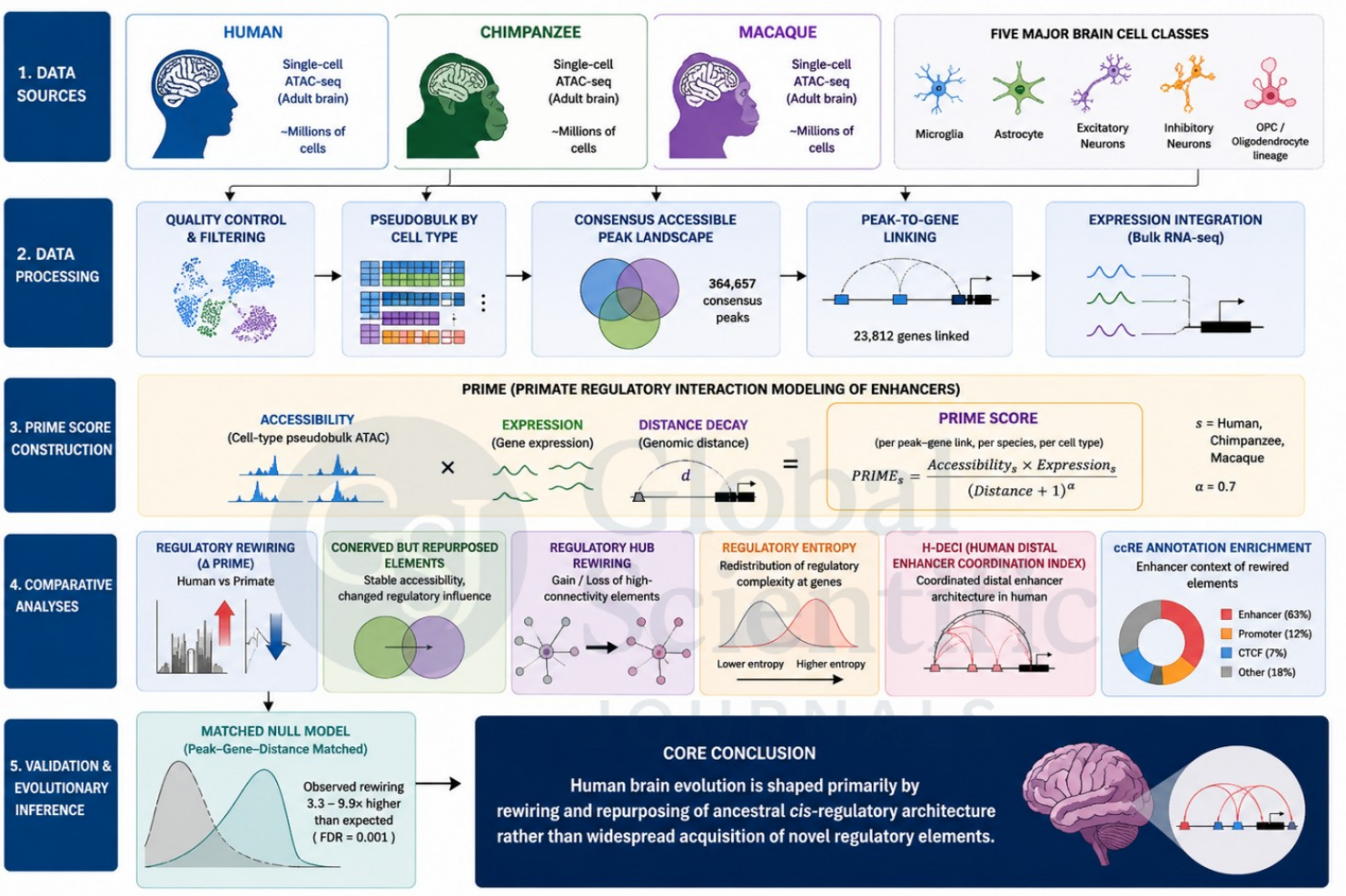

Figure 2. Cross-species chromatin accessibility divergence across major primate brain cell types. Stacked bars show the proportion of consensus accessible chromatin regions classified as conserved or small-change, human-gained accessibility, and human-reduced accessibility across five brain cell types. Accessibility landscapes remained predominantly conserved across species, with human-specific divergence representing a relatively small fraction of the total accessible regulatory space. Across

all lineages, human-reduced accessibility events occurred more frequently than human-gained events, indicating asymmetric regulatory divergence in the human brain.

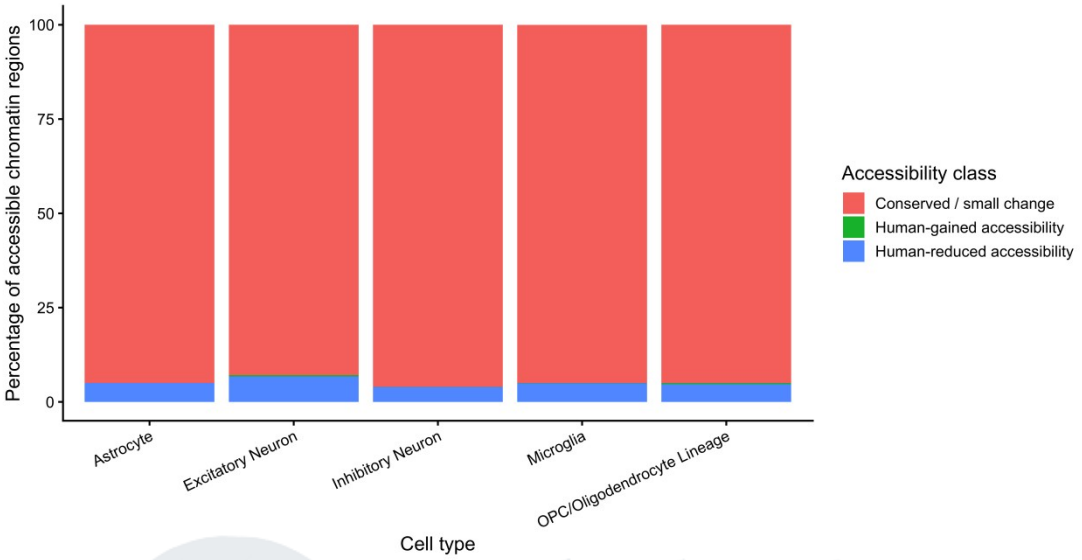

Figure 3. **Directional human-specific PRIME rewiring across major brain cell types.** Bars show the number of human-increased and human-reduced regulatory interactions identified using PRIME at the 95% empirical discovery threshold across five brain cell classes. Human-reduced regulatory coordination consistently dominated the rewiring landscape, whereas human-increased interactions occurred in smaller but lineage-specific subsets, particularly within OPC/Oligodendrocyte-lineage

and inhibitory neurons. These results indicate that human brain regulatory evolution is characterized primarily by redistribution and attenuation of coordinated cis-regulatory influence rather than widespread emergence of novel regulatory interactions.

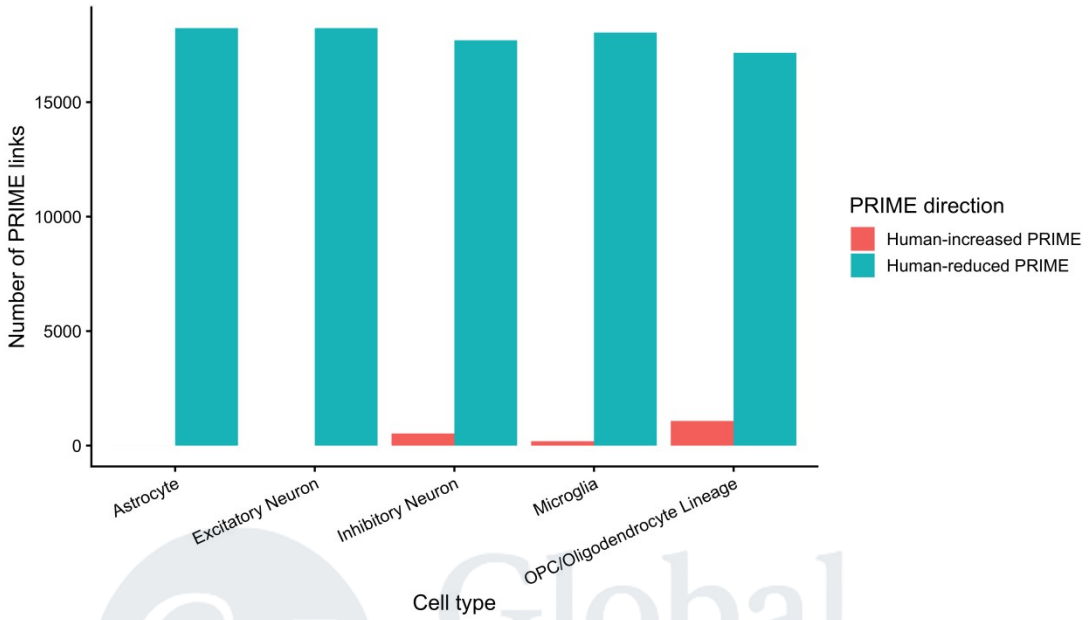

Figure 4. Enrichment of observed PRIME rewiring relative to biologically matched null expectations. Bars show the Null Enrichment Ratio (NER), calculated as the observed cumulative PRIME rewiring magnitude divided by the expected magnitude under matched null regulatory backgrounds controlling for accessibility,

expression, genomic distance, and regulatory annotation. Human-reduced rewiring exhibited consistently stronger enrichment than human-increased rewiring across most cell types, with Microglia and OPC/Oligodendrocyte-lineage cells showing the strongest deviations from null expectation. These results demonstrate that observed PRIME rewiring reflects structured evolutionary redistribution of regulatory coordination rather than stochastic properties of accessible chromatin architecture.

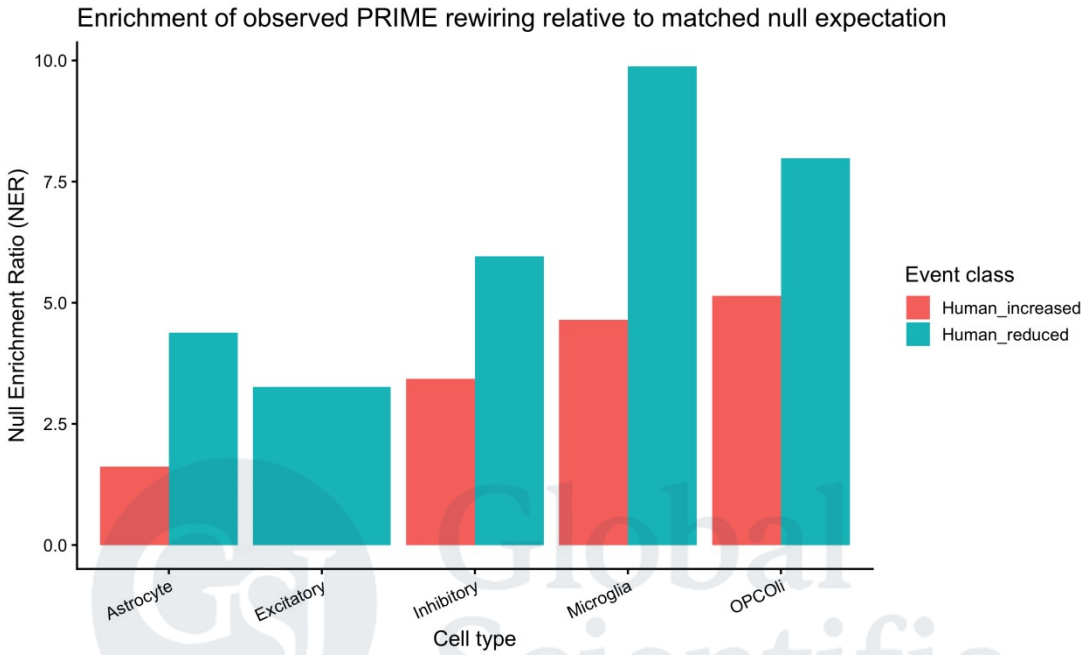

Figure 5. Enhancer-like elements dominate human PRIME rewiring architecture.
(A) Distribution of regulatory annotations across the shared cross-species accessible

chromatin landscape. Distal enhancer-like and intragenic regulatory elements comprised the majority of accessible regions, indicating that primate brain regulatory architecture is predominantly organized around enhancer-associated accessibility rather than promoter-centered regulation.

(B) Regulatory class composition of human-increased and human-reduced PRIME rewiring events at the 95% discovery threshold. Directional PRIME rewiring was enriched within enhancer-like regulatory contexts across multiple cell types, although promoter-associated and intragenic elements also contributed substantially to regulatory redistribution.

(C) Proportion of enhancer-like regulatory elements contributing to directional PRIME rewiring across brain cell types. Human-increased rewiring showed particularly strong enhancer enrichment in inhibitory neurons and OPC/Oligodendrocyte-lineage cells, supporting local repurposing of enhancer-associated regulatory architecture during human brain evolution.

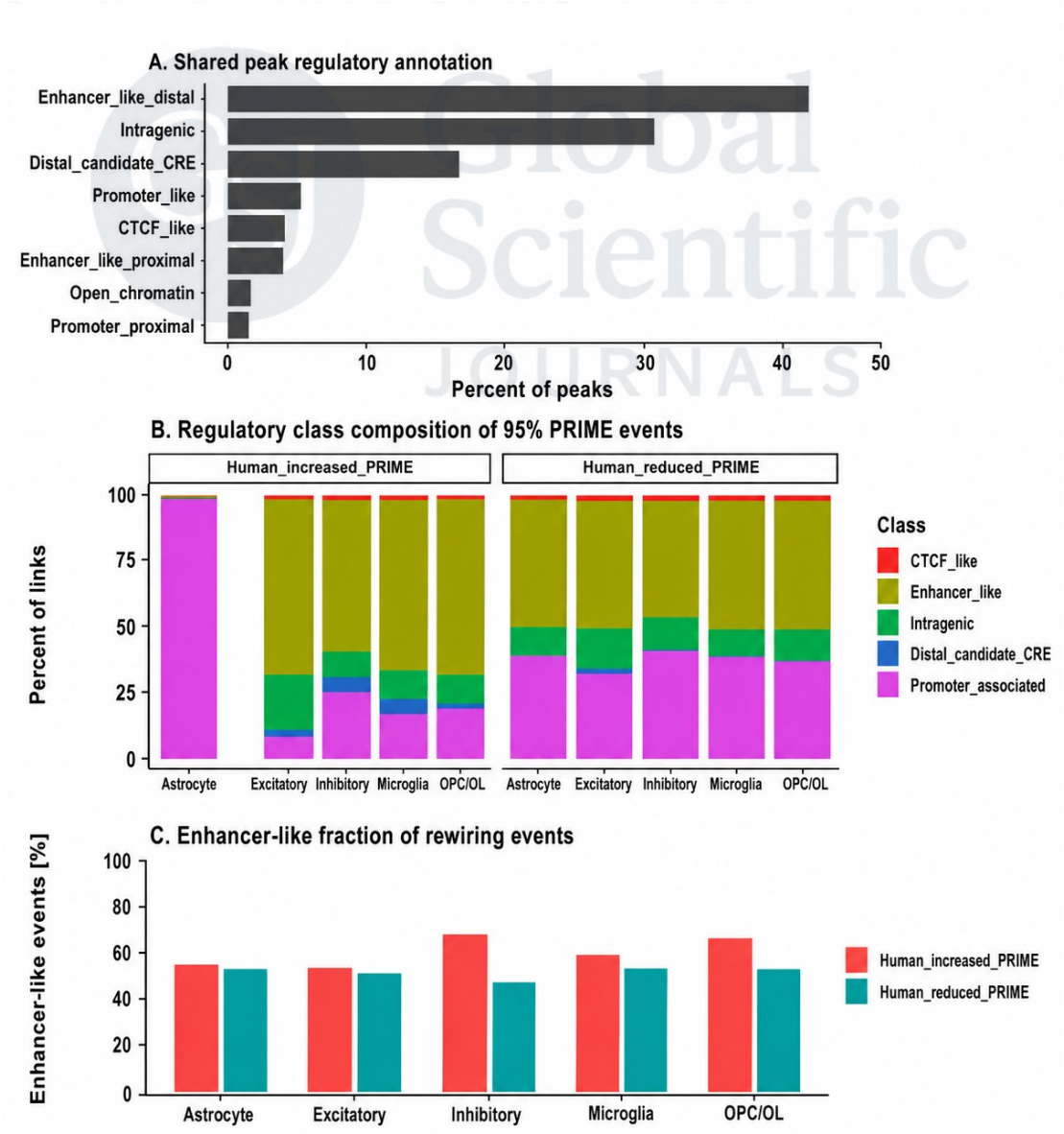

Figure 6. Regulatory entropy redistribution and conserved CRE repurposing across human brain cell types.
(A) Numbers of genes exhibiting human-expanded and human-contracted regulatory entropy across cell types. Entropy expansion consistently exceeded contraction, indicating selective broadening of coordinated regulatory influence in the human lineage.

(B) Conserved accessible regions exhibiting human-shifted PRIME coordination. Most conserved-repurposed events involved human-reduced regulatory coordination, demonstrating that evolutionary divergence frequently occurs through altered utilization of preserved regulatory architecture rather than changes in accessibility itself.

(C) Relationship between entropy expansion and conserved human-increased repurposing across cell types. Cell types with greater redistribution of regulatory coordination tended to show stronger evidence of regulatory repurposing, supporting coordinated remodeling of existing cis-regulatory networks during human brain evolution.

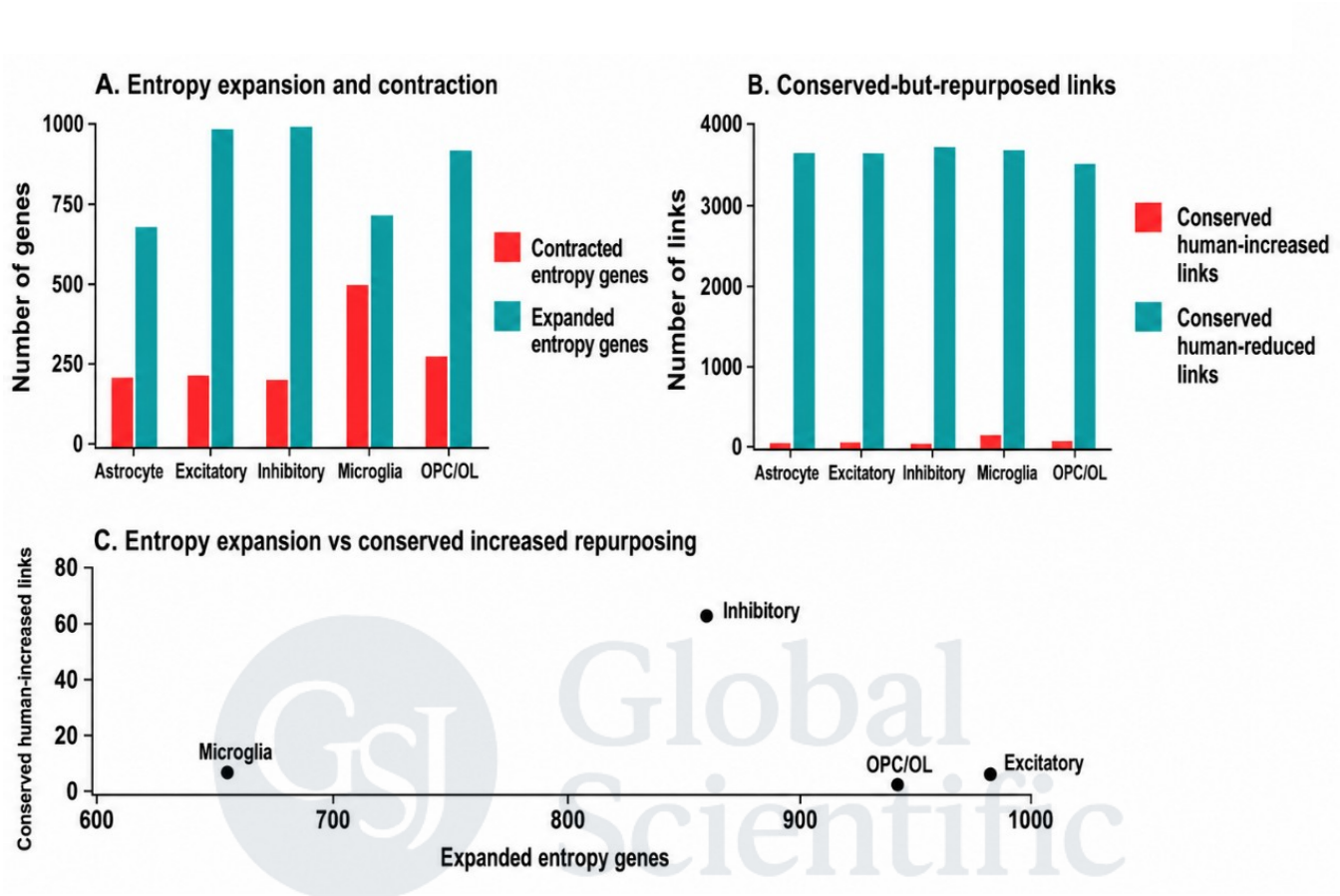

Figure 7. Recurrent human-specific PRIME rewiring genes across brain cell types.

(A) Recurrent human-increased PRIME genes across major brain cell classes. Dot size represents the magnitude of positive PRIME shift and color intensity indicates the maximum observed human-specific increase, highlighting genes that exhibit strengthened regulatory coordination across multiple lineages.

(B) Recurrent human-reduced PRIME genes across major brain cell classes. Dot size represents the magnitude of negative PRIME shift and color intensity indicates the minimum observed PRIME value, showing that human regulatory divergence more frequently occurs through attenuation and redistribution of coordinated cis-regulatory influence than through widespread regulatory gain.

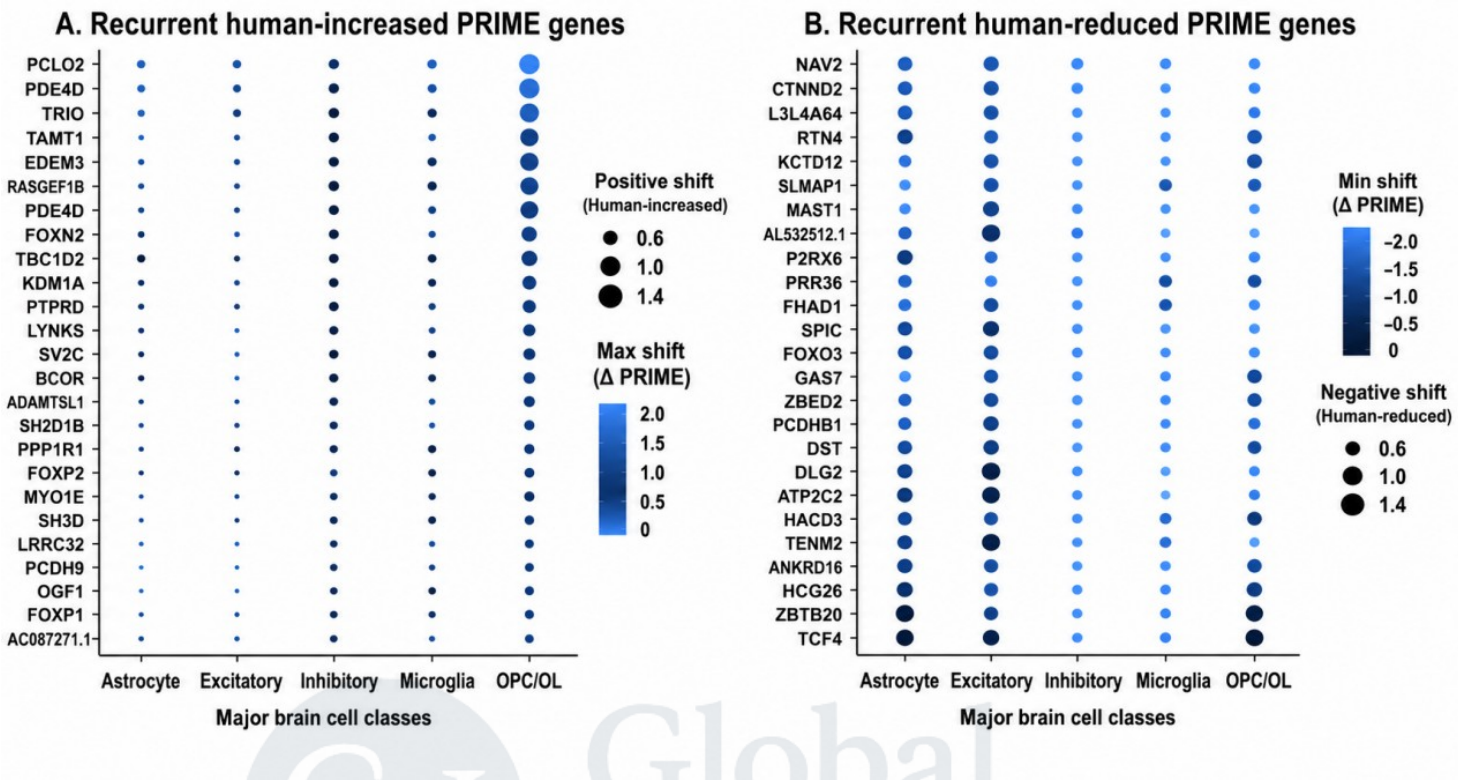

Figure 8. Human distal enhancer coordination converges on recurrent regulatory hub genes across brain cell types.

The figure shows recurrent genes exhibiting coordinated human distal enhancer architecture quantified using the Human Distal Enhancer Coordination Index (H-DECI). Dot size represents the number of coordinated distal enhancer links associated with each gene, while color intensity indicates H-DECI magnitude, reflecting the strength of coordinated enhancer influence. Genes including DLG2, PDE4D, TCF4, TRIO, PTPRD, DST, FOXP1, and ARID1B displayed recurrent high enhancer coordination across multiple lineages, indicating convergence of human regulatory evolution onto neurodevelopmental, synaptic, and transcriptional regulatory hubs rather than dispersed genome-wide enhancer activation.

